



ARCHIVES  
 of  
 FOUNDRY ENGINEERING

DOI: 10.1515/afe-2017-0051

Published quarterly as the organ of the Foundry Commission of the Polish Academy of Sciences



ISSN (2299-2944)

Volume 17

Issue 2/2017

55 – 62

# Friction and Wear Behavior of 201HT Cast Aluminum Alloy with Various Competitive Material

R. Li <sup>a,\*</sup>, L.J. Chen <sup>b</sup>, M. Su <sup>a</sup>, Q. Zeng <sup>c</sup>, H. Li <sup>a</sup>, Y. Liu <sup>b</sup><sup>a</sup> School of Big Data and Computer Science, Guizhou Normal University, Guiyang, Guizhou, China<sup>b</sup> College of Mechanical Engineering, Guizhou University, Guiyang, Guizhou, China<sup>c</sup> Guiyang Huaheng Mechanical Manufacture CO.LTD, Guiyang, Guizhou, China

\* Corresponding author. E-mail address lirong9242001@163.com

Received 07.02.2017; accepted in revised form 10.05.2017

## Abstract

The friction and wear properties of 201HT aluminum alloys and the corresponding competitive coupons were tested on an electro-hydraulic servo face friction and wear testing machine (MM-U10G). The microstructures of the competitive coupons were investigated by scanning electron microscopy (SEM) and consequently the corresponding friction and wear mechanisms were studied. The results demonstrated that: (1) the best competitive material of friction and wear performance of the 201HT was the 201HTC. (2) the 201HTC modified by carbon following the initial mill for oil storage of the micro-groove to be produced, increased the corresponding lubrication performance reduced the friction coefficient and wear rate effectively. (3) the 201HT-201HTC could obtain both better friction and wear mainly due to the initial process of grinding following the 201HT plastic deformation occurred in the surface and the formation of a series of re-melting welding points, whereas the 201HT material hardness would be similar to the 201HTC material hardness, which led into the competitive material friction and wear performance improvement.

**Keywords:** Casting aluminum alloy, Friction and wear, Competitive material

## 1. Introduction

Both the valve hole and the valve core of the hydraulic valve group would move relatively during utilization, which would result in wear in-between two components. If the friction and wear properties between the competitive materials are not suitable, that will lead the latter material to increase intermittently, which will result in an increased valve group leakage [1, 2]. Most existing hydraulic valve group materials utilized were the ductile iron and the steel (45#) as the valve body and core [3, 4]. The aluminum alloys are not utilized in the hydraulic multi-valve fabrication due to the corresponding low

strength, poor wear resistance, whereas only a proportion of the forged aluminum alloy is utilized in the relatively simple valve fabrication [5-8]. Though the forged aluminum alloys have enough strength, but it cannot withstand the complex internal flow of the hydraulic multi-valve.

In this project, specially prepared 201HT aluminum alloy materials were utilized in the hydraulic multi-way valve body manufacturing. It was necessary for the friction and wear properties of the valve hole and core pair material of the aluminum alloy hydraulic multi-way valve to be mastered during preparation and the best competitive material for the 201HT alloys to be obtained. Based on the comparative tests, the friction and wear status of 201HT aluminum alloys and various types of

aluminum alloys were obtained. Also, the friction and wear performance were compared to the existing valve group materials (ductile iron and 45 # steel), for an optimum competitive material for 201HT alloys to be obtained.

## 2. Experimental Procedure

### 2.1 Experimental methods

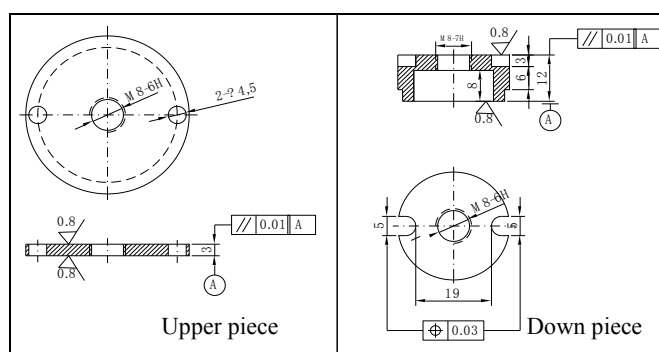
The friction and wear tester (MM-U10G) was utilized in the friction tests between the 201HT alloy and various materials. Also, the competitive material with a low coefficient of friction and less wear was selected. The competitive material was

prepared as presented in Figure 1 (a), which includes the upper and lower friction test pieces. These pieces were utilized in the friction tests and the data were recorder by the test machine as presented in Figure 1 (b).

### 2.2 Experiment execution

#### (1) Couple group design

For the friction and wear properties testing between the 201HT aluminum alloy, the carbon and the modified 201HT (abbreviated 201HTC), the RR350 alloy (abbreviated 350), the QT500 (abbreviated QT) and the 45# steel (abbreviated 45#) during actual experimentation, the wear material couple scheme of the test is presented in Table 1.



(a) Friction test pieces



(b) Test device

Fig. 1. Test pieces and device

Table 1.

Wear material couple group and other test parameters

Temperature	Force	Speed	Upper test piece	Down test piece
25 °C	180N	300rpm	201HTC	201HT
			350	201HTC
			45#	QT
			QT	201HTC
			201HT	201HTC

#### (2) Test procedure

1) First the upper test piece was installed and consequently the lower test piece was installed, whereas consequently the 46 # anti-wear hydraulic oil was added and the basic parameters were set.

2) The friction coefficient during testing was automatically recorded by the test machine, whereas the experiment parameters were recorded by the experiment software.

3) The Pre-wear pieces were required for 10 minutes, whereas consequently the test pieces were removed and washed (cleaned with acetone and alcohol), dried and weighed by an analytical balance and the weight was recorded.

4) Following the lower test piece assembly, the experiment started and the experiment parameters were recorded by computer software. The material wear (lower test piece) was measured every 15 minutes (The test piece wear was the difference between

the two weights).

5) The aforementioned 3-4 steps were repeated, whereas each sample group was tested for 60 minutes.

### 2.3 Alloy tissue test analysis

The surfaces of the finished specimens were observed by scanning electron microscopy (FEI-Quanta 400 FEG). The composition of the local particles was analyzed by energy dispersive X-ray microanalysis (EDAX).

### 3. Experimental results

#### 3.1 Analysis of friction coefficient and wear of different competitive materials

Figs.2 and 3 demonstrate the average friction coefficient and wear status for each pair of materials in 60 minutes.

The friction coefficient of each competitive material group had a downward trend as observed in Fig.2. The friction coefficient between the QT-45 # was the lowest and the friction coefficient was also stable. The friction coefficient of the QT-45 #

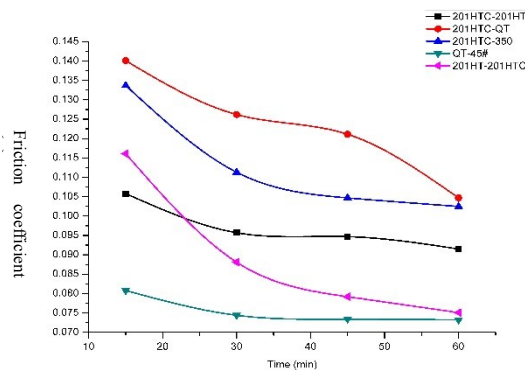


Fig. 2. Friction coefficient curve of competitive material

It could be observed from Fig.3 that the wear amount of each competitive material decreased as the wear continued. The 201HTC-QT wear was high at the beginning of wear. In contrast, the wear decrease was quite significant following a half-hour, which was close to the wear value of the other groups. The wear pattern of both 201HTC-QT and QT-45 # demonstrated a downward parabola (a wear minimum value exists) following 45 minutes, consequently the wear amount increased gradually. Although, both 201HTC-201HT and 201HTC-350 groups demonstrated opposite maximum wear values, followed by a gradually reduction in wear, or even a negative wear values. Wear amount of 201HT-201HTC is big in the initial state. It maintains a slow linear downward trend after 15 minutes.

was slightly higher than the aluminum alloy friction coefficient and the entire friction coefficient was lower than the aluminum alloy. Regarding the aluminum alloy friction couple, the 201HTC-QT dual friction coefficient was high, whereas the corresponding friction coefficient declined slowly. The 201HTC-201HT and the 201HTC-350 couples had similar friction coefficients. The friction coefficient of the 201HT-201HTC was higher at the early stage of wear, whereas the friction coefficient declined rapidly as the wear continued and gradually became stable between 0.075-0.080 at the later stage, which was the closest to the friction coefficient of the iron-carbon alloy. A good friction performance was reached.

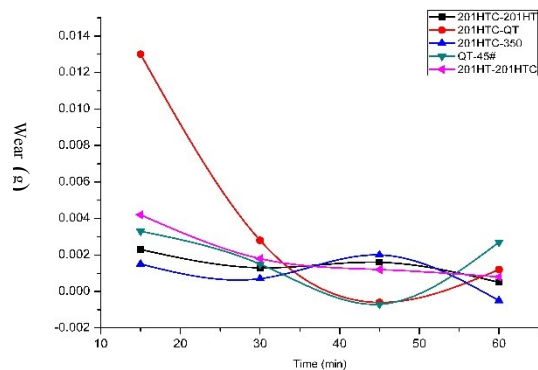
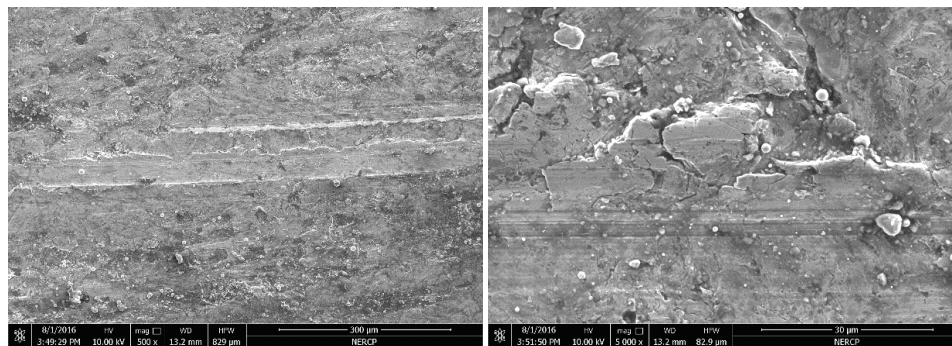


Fig. 3. Wear curve of competitive material

#### 3.2 Micro Morphology

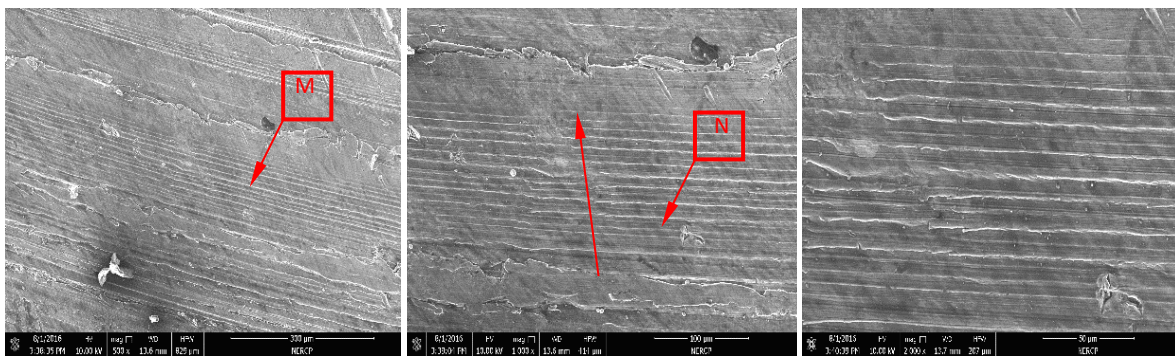
Figure 4 presents the QT surface scanning electron microscopy morphology (SEM) of the QT-45 # competitive material following 60 minute duration. The low power morphology of the QT surface morphology could be observed containing an amount of abrasive debris. Also, a high amount of shallow furrows and extrusions in the high power topography existed, which was mainly caused by the material plasticity slip.



(a) Low power (b) High power  
 Fig. 4. QT SEM of QT-45 # competitive material

Figure 5 presents the 201HTC specimen SEM that was the 201HTC-201HT competitive material following 60 minutes. The micro morphology was composed of a high number of parallel furrows and extrusion plastic deformation like stepped. Figure 5 (b) demonstrates an enlarged view of the M region of Figure 5 (a). From the morphology it could be observed that a release layer formed by the rolling repetition on the lower area. In the upper area of this figure, it could be observed that the alloy had an upward tendency by the square slipping. Some alloy was partially squeezed to the edge, which was possible for the broken cracks to be observed. It could also be noted that the direction of the slip band coincided with the direction of the centrifugal force of wear, as indicated by the arrows in Figure 5 (b). It was interpreted that the centrifugal force had a certain effect on the migration of the

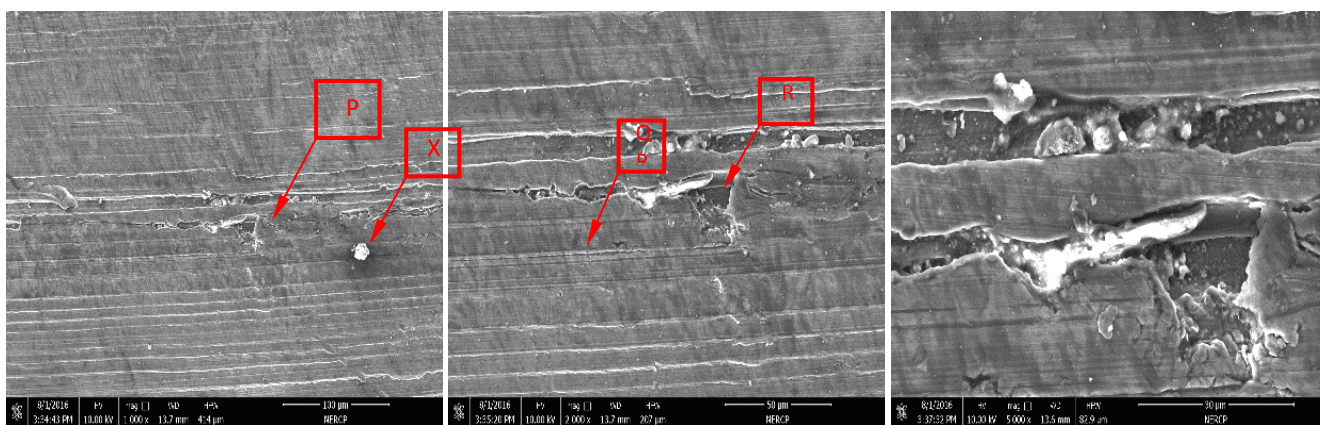
plastic deformation. Also, a further enlarged N zone could be observed as presented in Figure 5 (c). The parallel furrows were distributed and the edges of these furrows were metal fines from the repeated crushing. It occurred due to dual specimen rotation inadequate stability during wear, which resulted into a continuous swing on both surfaces of the dual pieces. This movement would roll these furrows continuously, resulting in the furrow edge formation of the metal from the parallel furrows under the action of alternating stress. Furthermore, a 20 $\mu$ m pit was formed in the lower right corner of Figure 5 (c). This pit might also be related to the alternating stress: the continuous alternating stress caused fatigue micro-cracks spreading on the surface, which could result in the peeling of the local material forming low-sized pits [9].



(a) Lower power (b) M area enlarged (c) N area enlarged  
 Fig. 5. 201HTC SEM of 201HTC-201HT competitive material

Figure 6 presents the SEM images of the 201HT specimen that was the 201HT-201HTC competitive materials following 60 minutes. It could be observed that besides the parallel furrows, a high number of deep furrows were present in the middle of the picture and deep low-sized pits existed in the local region as presented in Figure 6 (a). The broken cracks of plastic extrusion are presented in the Figure 6 (b), which was the P zone enlarged. Also, certain micro cracks appeared in the Q position. Figure 6 (c) presents the R zone enlarged figure of Figure 6 (c). A 10 $\mu$ m furrow and an irregular pit existed. Additionally, a high amount of

debris in both the furrow and the pit existed. The surface morphology of the 201HT might have occurred due to cut action and deep furrows formation by the hardness 201HTC. The plastic deformation aggravated on the surface due to the extrusion and temperature increase during dual wear, which led to micro defects shallow material aggravation. These defects were exacerbated by the inhomogeneous compressive alternating stress and formed as cracks within the surface layer. As the micro cracks spread and peeled off, a stepped pit morphology was formed, as presented in the figure.



(a) Lower power (b) P area enlarged (c) R area enlarged  
 Fig. 6. 201HT SEM of 201HT-201HTC competitive material

## 4. Results and Discussion

### 4.1 Friction coefficient impact of various competitive materials

In summary, it was demonstrated that the aluminum alloy friction coefficient was higher than the iron-carbon alloy from Fig. 2. In contrast, by the various friction coefficients comparison of the aluminum alloys, it could be observed that the friction coefficient of the 201HT-201HTC material was similar to the QT-45# in the following friction experiments, which provided an aluminum alloy utilization possibility instead of the ferroalloy manufacturing valve group.

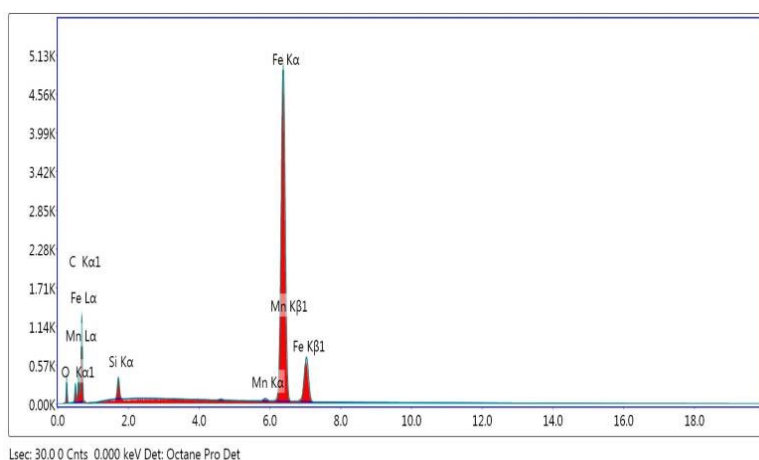


Fig. 7. EDAX of QT specimen

Element	Wt%	At%
C K	17.97	46.26
O K	4.99	9.64
Si K	2.61	2.87
Mn K	0.49	0.27
Fe K	73.95	40.95
Matrix	Correction	ZAF

It was indicated that a high amount of carbon existed on the QT surface following wear, actually playing a solid lubricating effect on wear. The spherical graphite could play a role in solid lubrication by friction reduction during wear, leading the two surfaces into dual wear to be easy and smooth. This carbon element declined the friction coefficient effectively.

Regarding the 201HT-201HTC competitive material, with a friction coefficient similarly to the ferroalloy, the friction coefficient was high in the initial stage. Although, subsequently to 30 minutes, the friction coefficient dropped sharply and the friction coefficient gradually became stable to a certain range. This process could be described as follows: During the initial stage of wear, the surface hardness of the 201HTC material was high following carbon modification, whereas the 201HT alloy surface was scratched. This would result in a high amount of furrows on the 201HT alloy surface. Also, as the dual wear continued, the surface layer of the soft material was gradually cut off and exposed to the hard phase of the alloy. These hard phases also produced furrows onto the 201HTC soft area. Subsequently, the peaks of the dual wear surfaces formed a support onto each other, which led the oil seep into a micro-groove cavity encircling the hard tissue. The lubrication increase between the wear specimens resulted in a gradual decline in the friction coefficient of the alloy. This process is presented in Figure 8.

The micro-grooves would form a certain pressure during dual

The main surface morphology of the QT-45 # was a shallow furrow. In the case of lubrication, the oil film could block the direct contact of the specimen pairs. Only certain scratches existed because of the rough peaks on the specimen. Due to 45 # steel being harder, the QT surface could be scratched and furrows were generated as the wear continued. Certain furrow cutting dusts would be attached onto the QT surface under high temperature. Also, other un-adhered dusts would flow onto the surface recessed area through the lubrication and fill the shallow pits. The interaction among furrows, iron filings and shallow pits formed continuously, which led to both lower friction coefficient and wear rate between the QT and the 45 #. In addition, the energy spectrum analysis of the QT specimen is presented in Figure 7.

wear, which would be transmitted onto the alloy surface and the alternating stress of the alloy material was intensified. The defects in the superfine material were aggravated, resulting in the surface micro-cracking and the material peeled off. The morphology of spalls could be observed in Figure 6 (c). From the specimen observations, these pits did not appear during the entire wear period. This occurred because the debris that generated the dual wear was removed from the wear area and a portion of the low-sized pieces fell into the pits under the pressure. Studies have shown that the alloy would be soft and melt in the high temperature and finally become welded [10]. This debris accumulated increasingly in the pit. The wear temperature would be high under the extrusion and re-melting and welding would form. The resulting morphology is presented in the X zone of Figure 6 (a).

Therefore, this system would form a dynamic equilibrium cycle of micro-pits generating, filled, and welding. The friction coefficient of the 201HT alloy would remain within a certain range finally. These welding points that were scattered on the surface played the role of hard points, which produced a support for the alloy dual wear. This led the friction coefficient of the competitive material to be gradually stabilized. If the hardness of the competitive material was quite different, the re-melting process would be substituted by adhesive friction, which would result in a high friction coefficient.

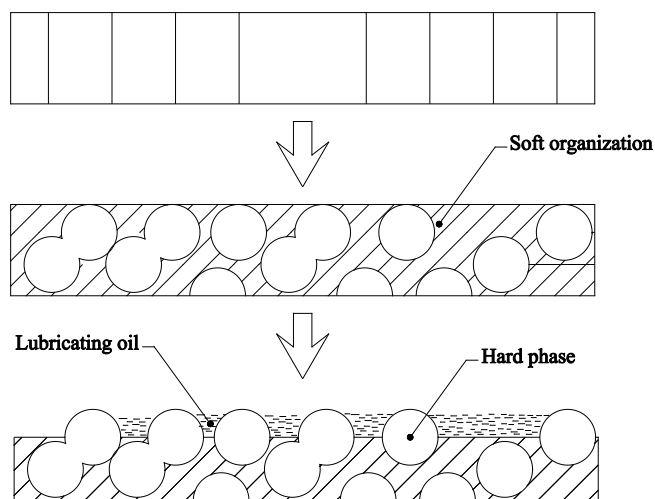


Fig. 8. 201HT-201HTC dual wear model

## 4.2 Wear impact of various competitive materials

The experimental results demonstrated that significant differences in the wear between the various competitive materials existed: the ferroalloy wear amount was lower than the aluminum alloy wear amount, whereas the aluminum alloy could produce a lower wear amount following an optimized combination than before. Compared to the wear curves of both QT-45 # and 201HT-201HTC alloys in Fig.3, it could be observed that the wear amounts of both alloys were similar. It was indicated that the wear resistance values of these aluminum alloys were nearly the same in performance to the ferroalloy materials. In contrast, the wear amount of the aluminum alloy was higher than the iron in the early stages of dual wear. Although as the wear duration continued, the wear amount of the aluminum alloy demonstrated a trend of linear decrease and the wear amount was stable. The ferroalloy wear value appeared low and consequently increased slowly.

The aluminum alloy was soft and the corresponding temperature diffusion was slow. Consequently, the specimen temperature increase was fast and the material plastic deformation was also serious, which led the adhesive wear to be serious during the initial stage of dual wear. Hard spots formed following the phenomenon of "re-melting and welding" as aforementioned, which could enhance the micro hardness of the surface [11]. This would constitute the hardness values of the 201HT and the 201HTC to be similar and prevent the adhesion cutting by the hard alloy, consequently reducing the amount of wear.

Regarding the ferroalloys, certain rough peaks existed on the two surfaces at the beginning of wear. These rough peaks would produce furrows on the surface, resulting in high initial wear. When these peaks became smooth following the experiment, the system would form a quite high quality of the grinding surface with the oil film and the spherical carbon lubrication. A quite low wear for the ferroalloy would appear.

Regarding the 201HTC-QT wear significant reduction, it was probably due to the iron alloy displaying higher hardness than the

201HTC, which made all uneven surfaces of the 201HT polished by wear. This process mainly demonstrated adhesion wear and the wear amount was also high. Following the experiment execution, the 201HTC surface could sustain a certain plastic deformation and certain hard spots were exposed. Also, both the 201HTC and iron contained a certain carbon element, which could be resulted from solid lubrication and constitute the wear and materials removal to be significantly decreased. As the friction and wear continued, the 201HTC alloy wear was increased due to the surface temperature increase and the lubrication oil film failure on both surfaces, which aggravated the plastic deformation and wear adhesion of the 201HTC alloy.

## 4.3 Hardness difference impact on friction and wear

The friction and wear of the alloy performance was related to the surface hardness and the hardness differences of the alloy. Table 2 presents the hardness of the material and the differences between the hardness values of values materials. From this table, positive and negative hardness difference existed: a positive value was interpreted that the upper piece was harder than the lower piece. It could be observed that a positive friction coefficient could lead to a lower friction coefficient of the competitive material, whereas a negative hardness difference displayed a higher friction coefficient according to the friction coefficient curves of Figure 2. Also, the higher negative value would lead to higher friction coefficient. The adhesion friction theory that was put forward by the Tabor and Bowden, pointed that the friction was the resistance sum of both the adhesive and furrow effects. Moreover, the friction force in the furrow was inversely proportional to the square root of the soft material yield (the harder the material, the lower the furrow force) [12].

Due to the aluminum alloy was relatively soft, a high difference hardness of the alloy between the dual materials would lead in the furrow formation on the alloy surface. The higher the hardness difference between the dual materials, the furrow force

would produce higher impact on the soft materials. Additionally, the hard material would be adhered by the soft material following a certain period of time and formed a thin film on the surface,

which would reduce the friction coefficient between the dual wear materials.

Table 2.  
Hardness and hardness differences of dual wear materials

Material (Upper piece)	Hardness(HBS) (Lower piece)	Dual material	Hardness difference* (HBS)
45#	About 580(HRC50)	QT-45#	273
QT	213	201HTC-QT	77
201HTC	136	201HTC-201HT	-11
201HT	129	201HTC-350	-29
350	107	201HT-201HTC	9

\*Note: Hardness difference=upper piece hardness- lower piece hardness

As presented in Fig.2 (blue and black curves), the negative hardness difference wear curves all first declined, consequently gradually increased and finally decreased gradually. The higher negative difference had a lower wear amount. When the specimen had a high negative difference, the hardness of the material was less affected by both furrow and adhesion, which would lead to a lower wear amount. Following the initial dual wear, the soft material would be adhered to the surface of the hard material. These attachments would be "re-welded" and adhere onto the hard surface. This would lead the hard material to form the adhesion wear, also observed in the wear curve that gradually increased.

As the adhesion wear tended to be stable, the soft material adhesive transfer and these materials would be attached onto the hard alloy surface, leading the wear of the alloys to be decreased.

Therefore, the hardness differences had a higher impact on the alloy friction coefficient and wear rate: the positive hardness difference could produce a lower friction coefficient, whereas the negative hardness difference led into a lower amount of wear formation.

## 5. Conclusions

From the analysis of the aforementioned test results, the following conclusions were drawn:

(1) The friction and wear properties of the 201HT-201HTC dual material displayed good friction and wear properties. The soft alloy material (201HT) sustained plastic deformation and formed re-melting welding points on the dual wear surface, which made the hardness of the 201HT to be similar to the 201HT. Finally, the friction coefficient and wear amount of the 201HT-201HTC dual material decreased gradually.

(2) The hardness differences of the aluminum alloy dual materials should not be quite high: the dual group should pass through initial hardening and the actual hardness of the soft alloy surface should be similar to the hardness of the hard material, which would lead in both the friction coefficient and wear amount stability.

## Acknowledgments

This research was financially supported by the Industrial

Research Projects of Guizhou Province, China (GZ NO.[2015]3004). Moreover, this research was also financially supported by the Guizhou Science and Technology Cooperation Plan, Guizhou, China (LH No. [2016]7222) and the Guizhou Science and Technology Innovation Talent Team, Guizhou, China [(2014) 4013]. This research is also support by Doctoral Research Foundation of Guizhou Normal University (2017).

## References

- [1] Gao, X.Y., Wu, Z.Y., Zhang, X.L., Liu, Y.H. & Qu, J.T. (2013). Design of water-based high-speed on-off valve spool and its sealing. *Lubrication Engineering*. 38(9) (Sept.), 50-53. DOI: 10.3969/j.issn.0254-0150.09.012.
- [2] Wu, L., Yang, S.D., Liu, S.Y. & Wei, M. (2012). Wear life prediction for a large diameter spool valve. *Machinery Design & Manufacture*. 8 (Aug.), 234-236.
- [3] Pang, G.Z., Qi, L.H., Fu, Y.W., Fei, J. & Zhang, X. (2012). Wet friction and wear behavior of graphite-filled carbon fabric composites. *Tribology*. 32(4) (July.), 50-53.
- [4] Wang, S.R., Liu, Y.L., Zhu, Y.H., Guo, P.Q. & Wang, M. (2013). Microstructure and mechanical properties of cast iron for cartridge valve. *Foundry Technology*. 34(10), (Oct.), 1272-1274.
- [5] Wang, M.F., Wang, F. & Guo, X. (2011). Solution of shrinkage for triple plate valve body. *Foundry Equipment and Technology*. 2 (Apr.):31.
- [6] Li, B., Qu, S.G., Zhao, X.H., Tang, S.T. & Li, X.Q. (2014). Numerical simulation research for casting process of integral multi-way valve body. *Foundry*. 63(10), (Oct.), 1014-1018.
- [7] Wen, H.L., Shen, R.H. & Wu, Y.W. (2014). Simulation and optimization of solidification process for large integral multiway valve body. *Foundry Technology*. 35(1), (Jan.), 182-184.
- [8] Song, L.M. & Huang, H. (2014). Simulation research on casting process for nuclear grade butterfly valve body. *Foundry Technology*. 35(4), (Apr.), 829-831.
- [9] Cheng, S.Y., Liu, J.H., Guo, J., Wang, W.J. & Liu, Q.Y. (2015). Effect of wheel material characteristics on wear and fatigue property of wheel-rail. *Tribology*. 35(5) (Sept.):531-537. DOI: 10.16078/j.tribology.2015.05.003.
- [10] Wen, S.Z. (1990). *Tribological Theory*. Beijing: Tsinghua

- University Press. 01:314.
- [11] Tian, Y.H., Yang, S.H., Wang, C.Q., Wang, X.L. & Lin, P.R. (2015). Volume effect of shear fracture behavior of Sn3.0Ag0.5Cu/Cu lead-free solder joints, *Acta Metallurgica Sinica*. 46(3), (Mar.), 366-371.
- [12] Bowden, F.P., Tabor, D. (1982). *Solid friction and lubrication*. Beijing: Machinery Industry Press, 11.